Exact gradient flow and saddle points in lattice fermion models

Maksim Ulybyshev,
Universität Würzburg, Germany
maksim.ulybyshev@physik.uni-wuerzburg.de

in collaboration with:
Fakher Assaad, Savvas Zafeiropoulos, Christopher Winterowd

Partially published in:
PRD 101, 014508 (2020)

Lefschetz thimbles decomposition

$$\mathcal{Z} = \int_{\mathbb{R}^N} \mathcal{D}\Phi \, e^{-S[\Phi]} = \sum_{\sigma} k_\sigma \mathcal{Z}_\sigma$$

$$\mathcal{Z}_\sigma = \int_{\mathcal{I}_\sigma} \mathcal{D}\Phi \, e^{-S[\Phi]}$$

Saddle point: $$\left.\frac{\partial S}{\partial \Phi}\right|_{\Phi = z_\sigma} = 0$$

Gradient flow equations: $$\frac{d\Phi}{dt} = \overline{\frac{\partial S}{\partial \Phi}}$$

$$\mathcal{Z} = \sum_{\sigma} k_\sigma e^{-i \, \mathrm{Im}\, S(z_\sigma)} \int_{\mathcal{I}_\sigma} \mathcal{D}\Phi \, e^{-\mathrm{Re}\, S(\Phi)}$$

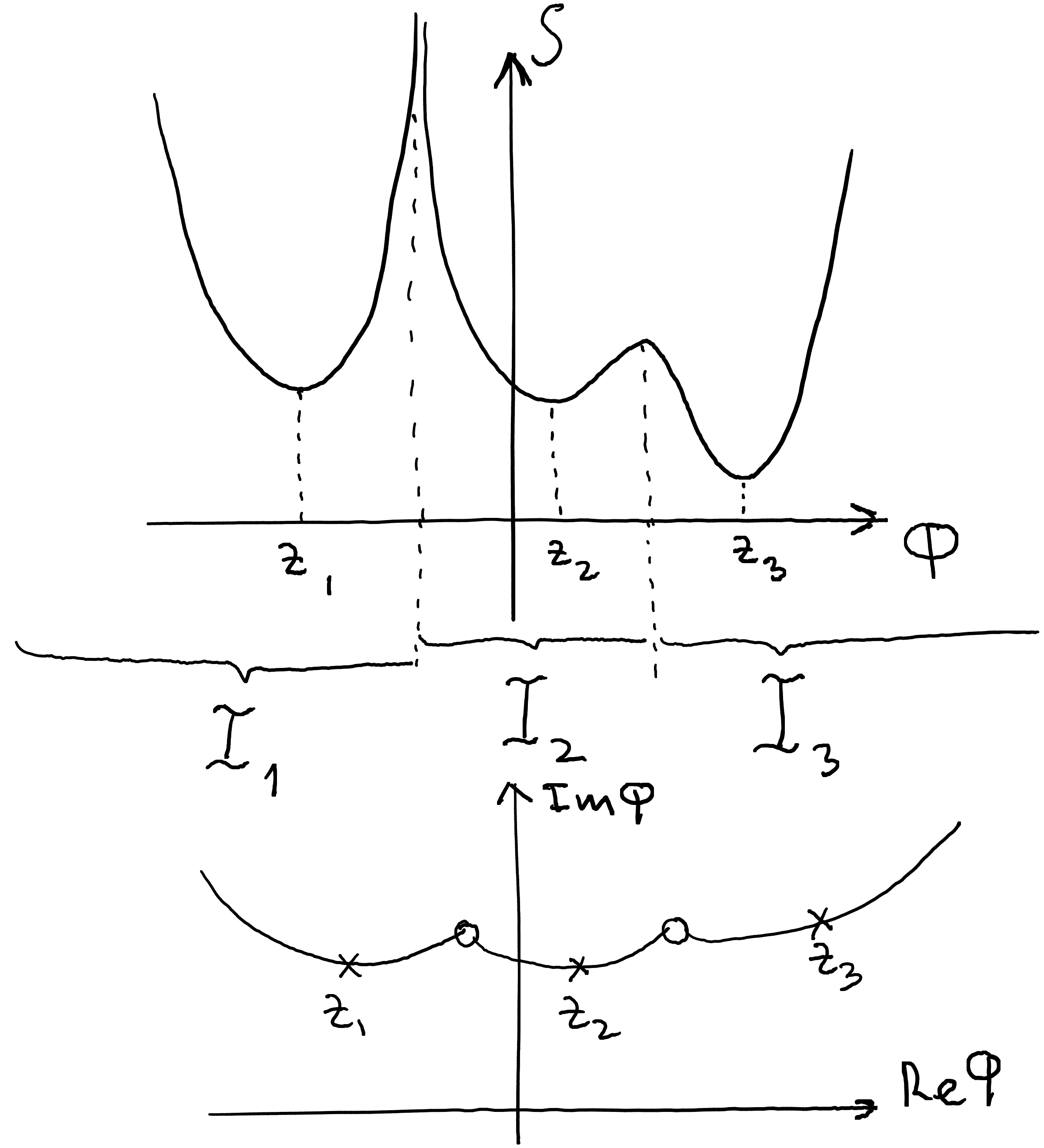

We will demonstrate that it is possible to find all important saddle points of generic model with lattice fermions. Subsequently, we construct the quasi-classical approximation to the partition function by adding gaussian fluctuations around these saddles. We will demonstrate connection of these saddle points to conventional instantons, and discuss the implications for the sign problem (Scaling of the number of thimbles in the thermodynamic limit: one- or many-thimble regime?).

We also discuss, which physical phenomena can be described by this saddle points approximation (with the special emphasis on the spontaneous symmetry breaking, where fermions acquire mass gap).

Exact calculation of fermonic forces

$$S = S_b + \ln \det M \qquad \Longrightarrow \qquad \frac{d\Phi}{dt} = \overline{\frac{\partial S}{\partial \Phi}}$$

Calculation of the derivatives of fermionic determinant is based on the representation:

$$\overline{M}^{st}(U) = \begin{pmatrix} 1 & D_1 & 0 & 0 & 0 & \dots \\ 0 & 1 & D_2 & 0 & 0 & \dots \\ 0 & 0 & 1 & D_3 & 0 & \dots \\ 0 & 0 & 0 & 1 & D_4 & \dots \\ \vdots & & & & \ddots & \\ -D_{2N_\tau} & 0 & 0 & & \dots & 1 \end{pmatrix}$$

$$\overline{M}^{st\,-1}(U) = \begin{pmatrix} g_1 & \dots & \dots & \dots & \dots & \bar{g}_{2N_\tau} \\ \bar{g}_1 & g_2 & \dots & \dots & \dots & \dots \\ \dots & \bar{g}_2 & g_3 & \dots & \dots & \dots \\ \dots & \dots & \bar{g}_3 & g_4 & \dots & \dots \\ \vdots & & & & \ddots & \\ \dots & \dots & \dots & & \dots & g_{2N_\tau} \end{pmatrix}$$

Possible for Staggered fermions [Nuclear Physics B 371, 539 (1992)], Wilson fermions, and general tight-binding lattice models in condensed matter physics

Derivative:

$$\frac{\partial \ln \det M}{\partial \Phi} = \mathrm{Tr}\left(M^{-1} \frac{\partial M}{\partial \Phi} \right)$$

Elements of fermionic propagator are computed through the iterations

$$\bar{g}_{i+1} = D_{i+1}^{-1} \bar{g}_i D_i$$

$N_s^3 N_\tau$ - scaling

«seed» blocks for iterations - from Schur complement solver [arXiv 1803.05478]

Recovering exact saddle points from Hybrid Monte Carlo data

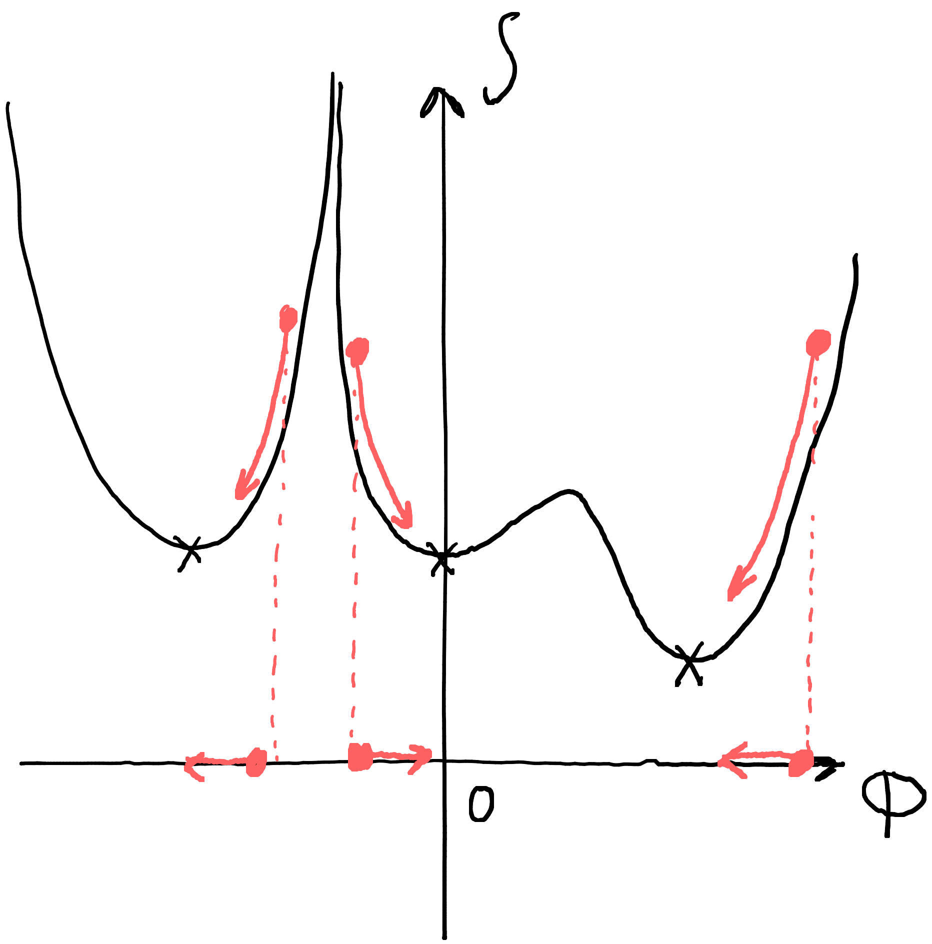

Final histogram shows $\frac{Z_\sigma}{Z}$ shares

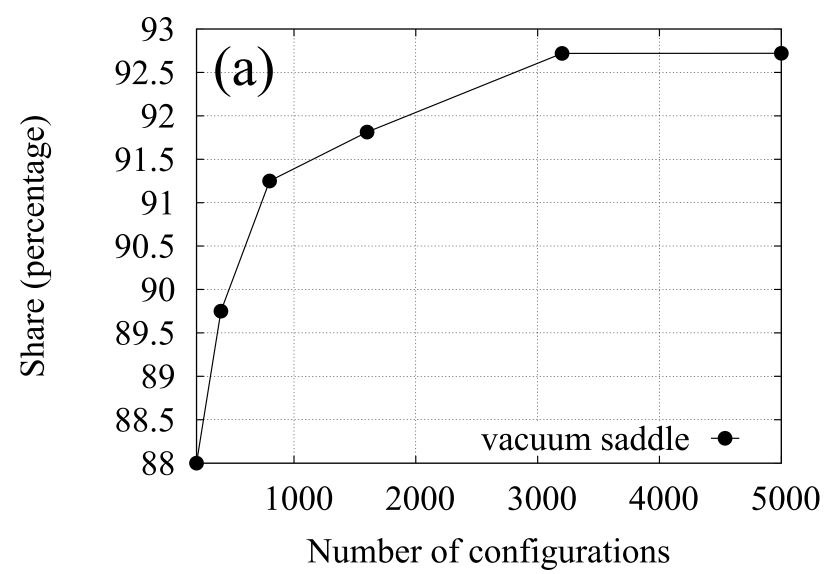

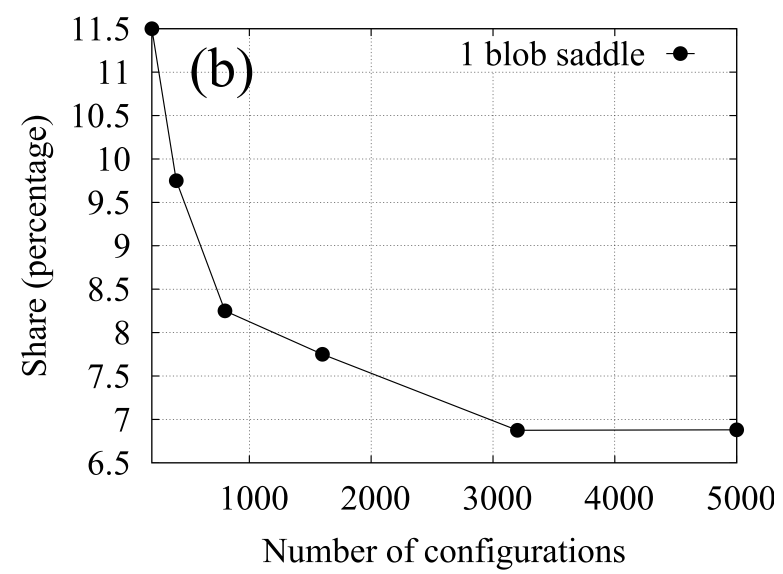

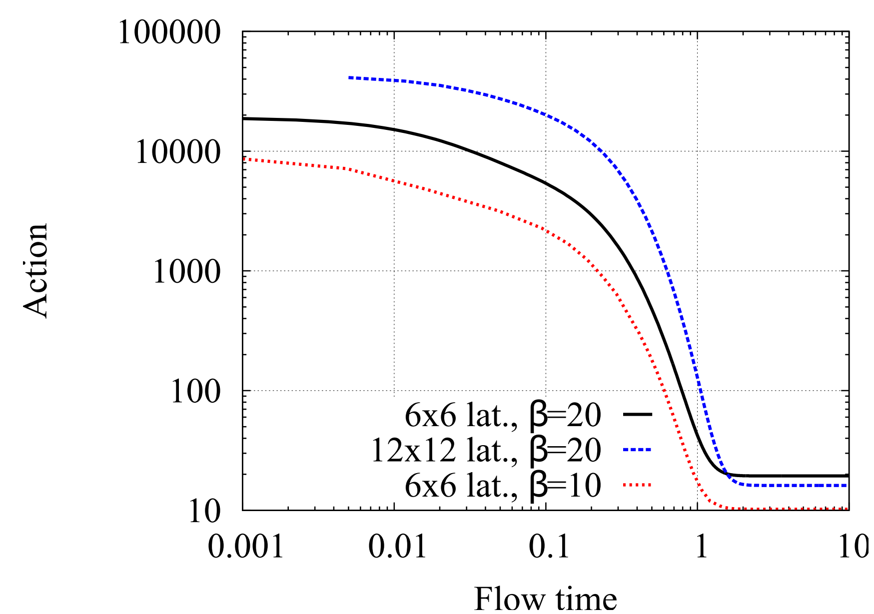

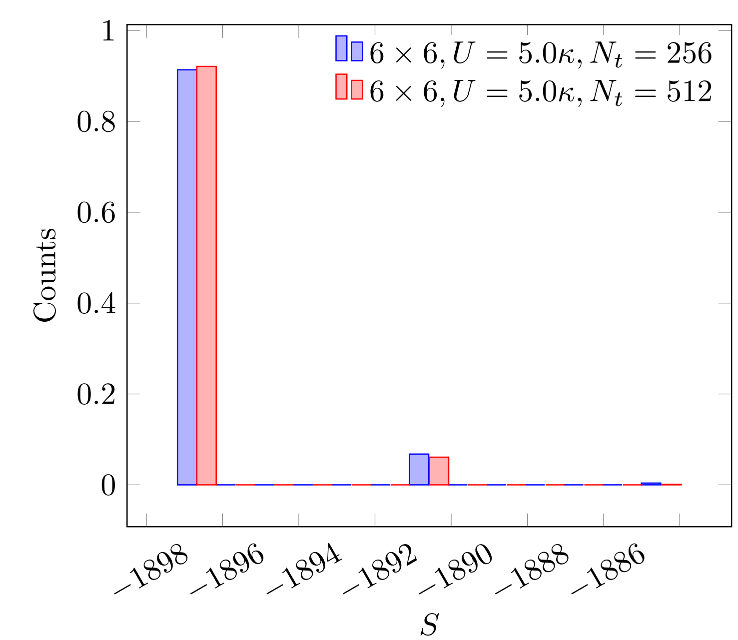

Hubbard model on hexagonal lattice

$$\hat{H} = -\kappa \sum_{\langle x,y \rangle,\sigma} \left(\hat{c}^\dagger_{x\sigma}\hat{c}_{y\sigma} + h.c.\right) + U\sum_x \hat{n}_{x\uparrow}\hat{n}_{x\downarrow} - \left(\frac{U}{2} - \mu\right)\sum_x \left(\hat{n}_{x\uparrow} + \hat{n}_{x\downarrow} - 1\right)$$

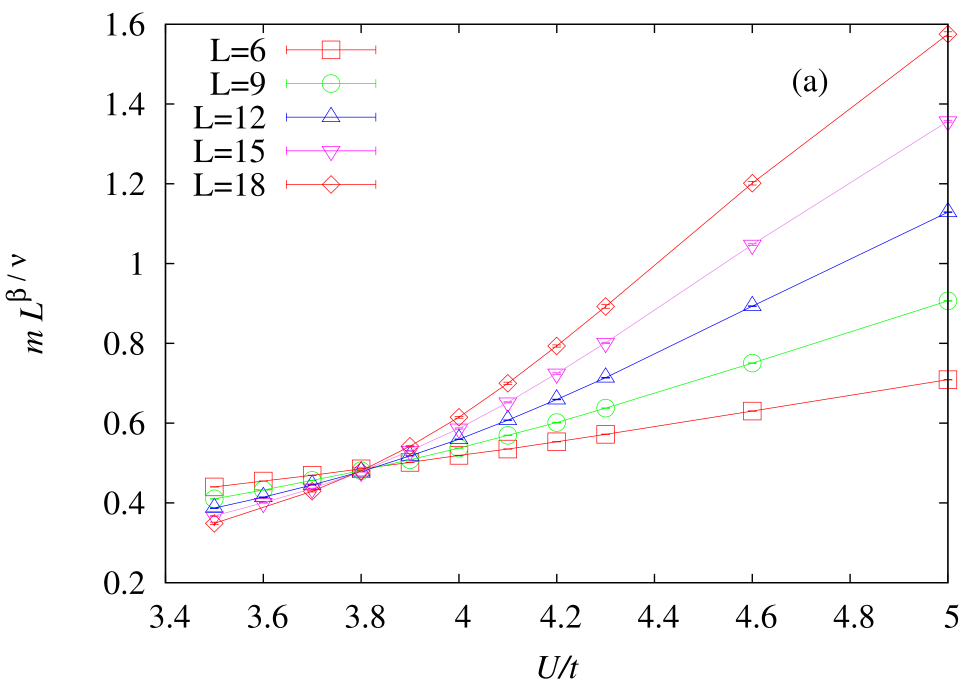

Semi-metal - AFM insulator transition at U=3.8 κ

F. Assaad, I. Herbut, PRX, 3, 031010 (2013)

$$\mathcal{Z} = \mathrm{Tr}\, e^{-\beta\hat{H}} \approx \mathrm{Tr}\, \left(e^{-\delta\hat{H}_{(2)}} e^{-\delta\hat{H}_{(4)}} e^{-\delta\hat{H}_{(2)}} e^{-\delta\hat{H}_{(4)}} \ldots\right)$$

$$\frac{U}{2}(\hat{n}_{el.} - \hat{n}_{h.})^2 = \frac{\alpha U}{2}(\hat{n}_{el.} - \hat{n}_{h.})^2 - \frac{(1-\alpha)U}{2}(\hat{n}_{el.} + \hat{n}_{h.})^2 + (1-\alpha)U(\hat{n}_{el.} + \hat{n}_{h.})$$

$$e^{-\frac{\delta}{2}\sum_{x,y} U_{x,y}\hat{n}_x\hat{n}_y} \cong \int D\phi_x e^{-\frac{1}{2\delta}\sum_{x,y}\phi_x U^{-1}_{xy}\phi_y} e^{i\sum_x \phi_x \hat{n}_x},$$

$$e^{\frac{\delta}{2}\sum_{x,y} U_{x,y}\hat{n}_x\hat{n}_y} \cong \int D\phi_x e^{-\frac{1}{2\delta}\sum_{x,y}\phi_x U^{-1}_{xy}\phi_y} e^{\sum_x \phi_x \hat{n}_x}$$

$$\boxed{\alpha = 0 \ldots 1}$$

Fierz identities:

$$\delta^a_b\delta^c_d = \frac{1}{2}\delta^a_d\delta^c_b + \frac{1}{2}\sum_i \sigma^{(i)a}{}_d \sigma^{(i)c}{}_b$$

$$\left(\bar{a}O_i b\right)\left(\bar{c}O^i d\right) = \sum_k C_{ik}\left(\bar{a}O_k d\right)\left(\bar{c}O^k b\right)$$

$$\mathcal{Z}_c = \int \mathcal{D}\phi_{x,\tau}\,\mathcal{D}\chi_{x,\tau}\, e^{-S_\alpha} \det M_{\mathrm{el.}} \det M_{\mathrm{h.}},$$

$$S_\alpha[\phi_{x,\tau},\chi_{x,\tau}] = \sum_{x,\tau}\left[\frac{\phi^2_{x,\tau}}{2\alpha\delta U} + \frac{(\chi_{x,\tau} - (1-\alpha)\delta U)^2}{2(1-\alpha)\delta U}\right]$$

$$M_{\mathrm{el.,h.}} = I + \prod_{\tau=1}^{N_\tau}\left[e^{-\delta(h\pm\mu)}\mathrm{diag}\,\left(e^{\pm i\phi_{x,\tau} + \chi_{x,\tau}}\right)\right]$$

Examples of the saddles for the Hubbard model on hexagonal lattice

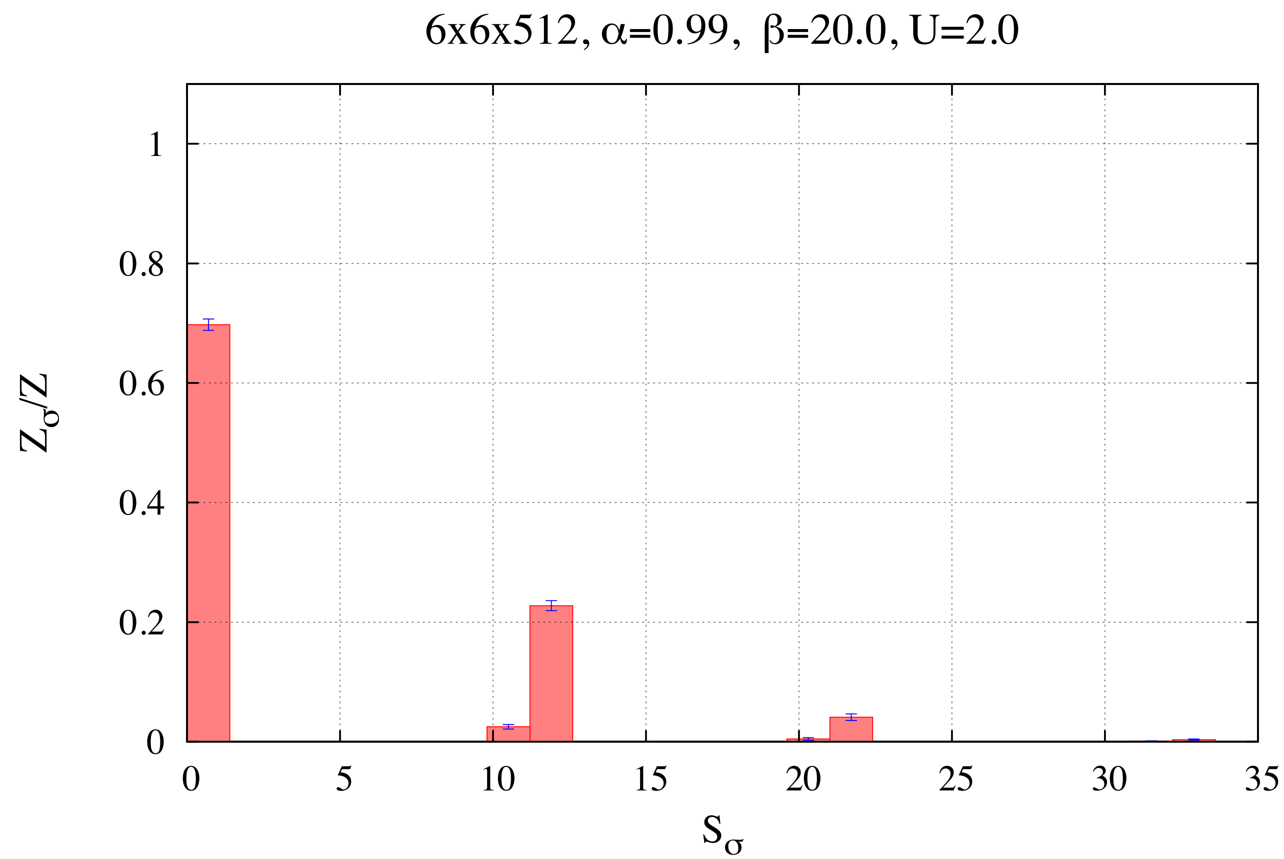

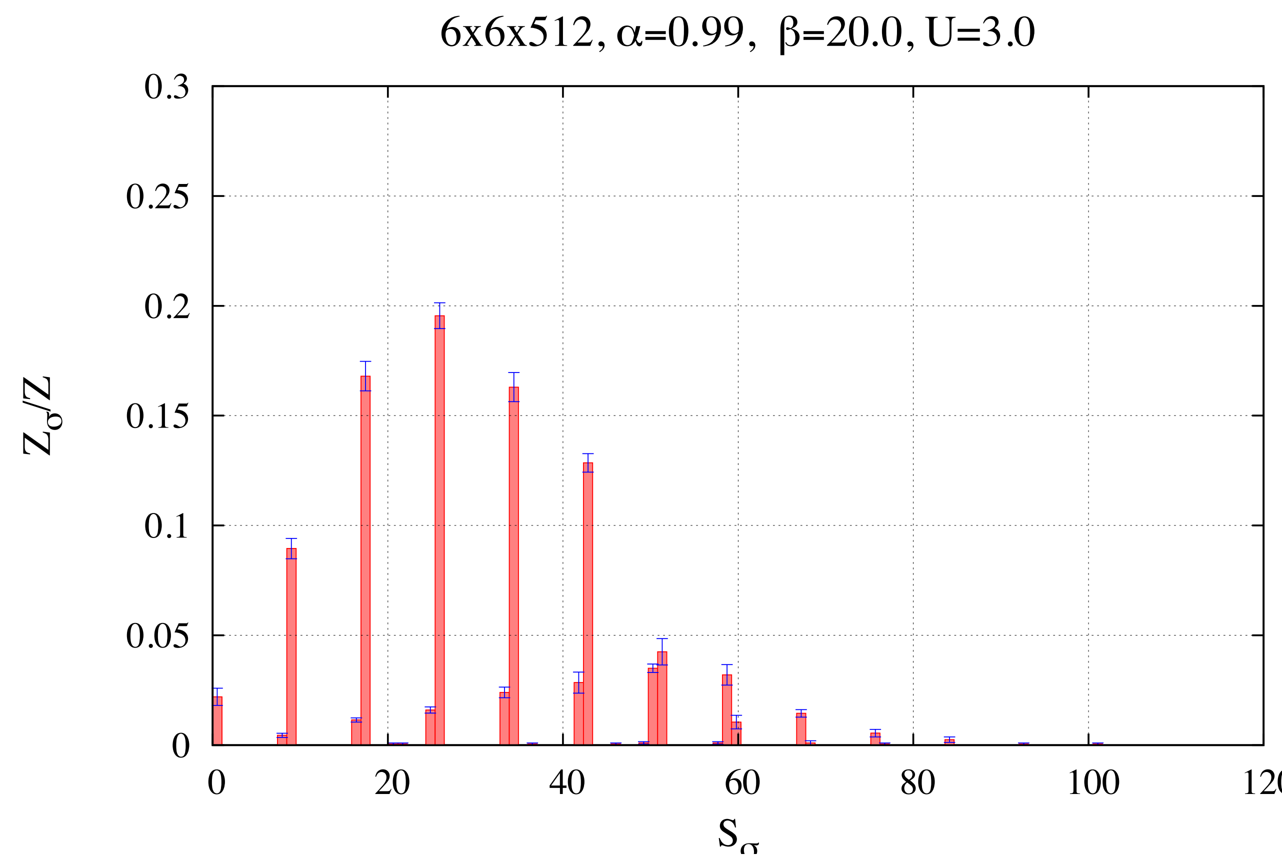

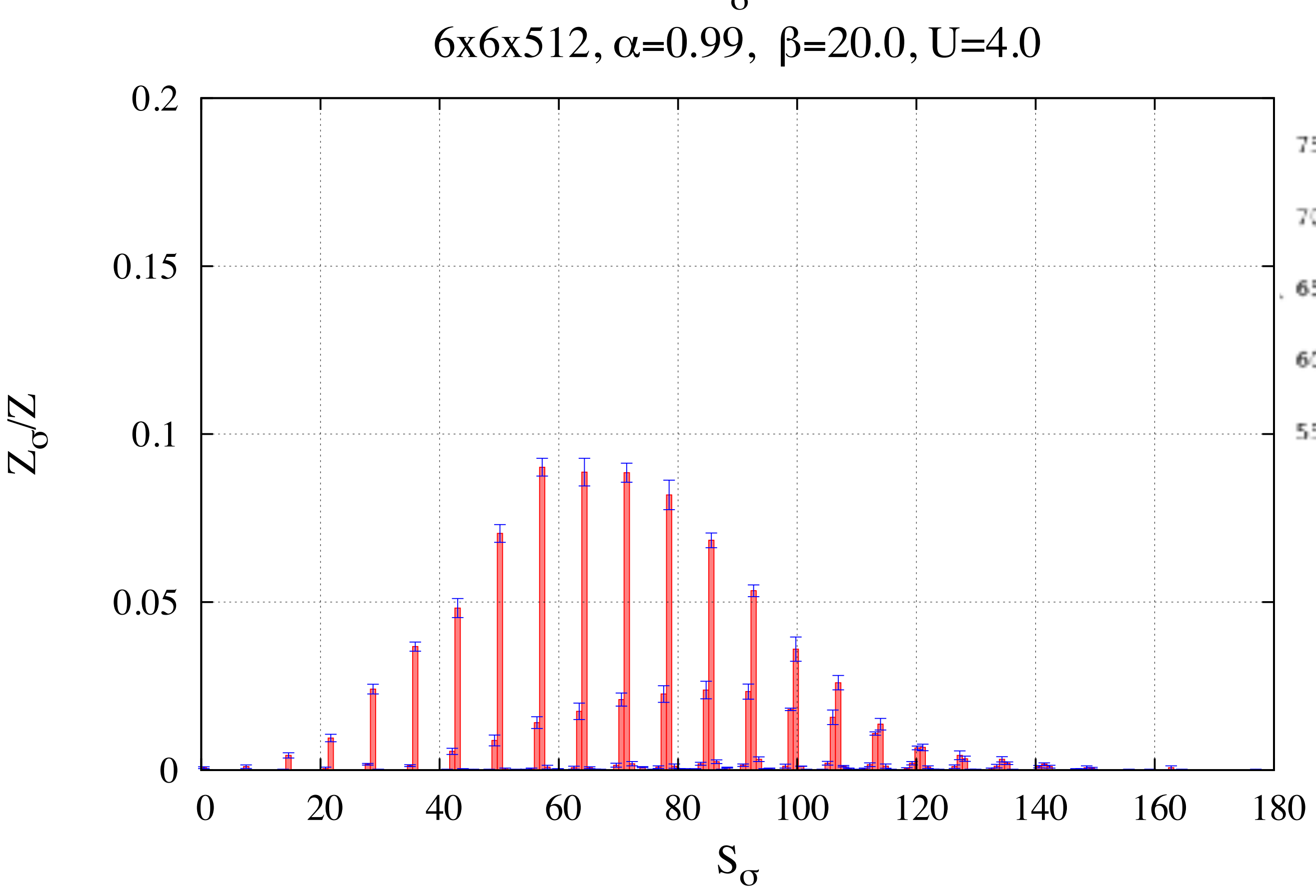

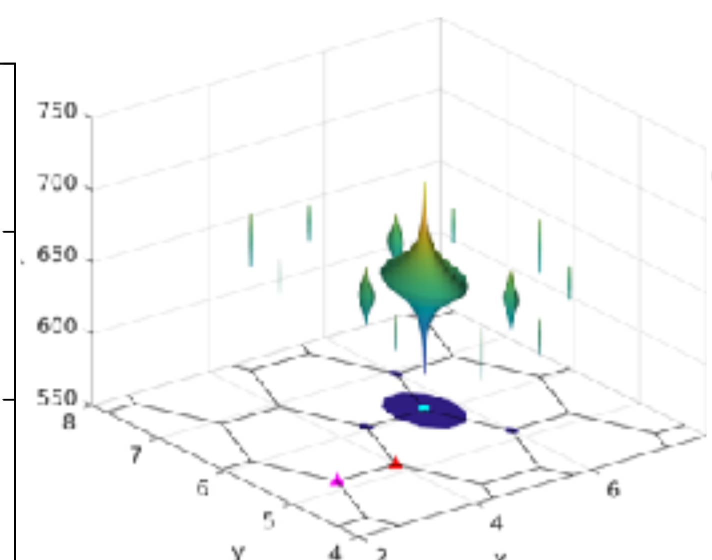

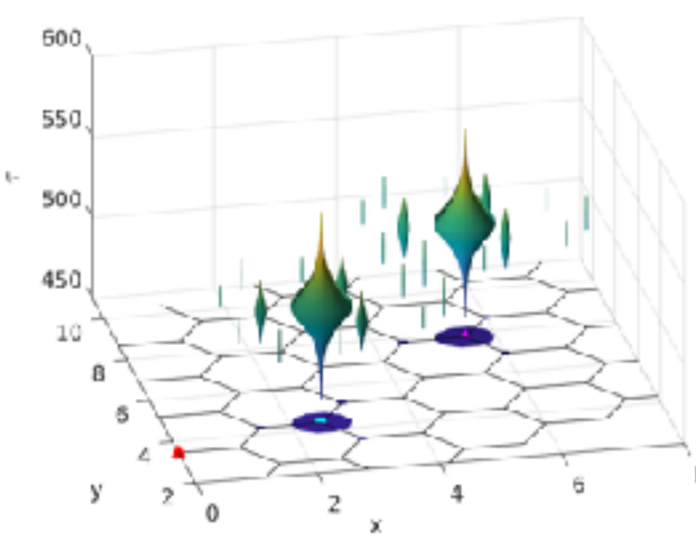

Saddle point field configurations are localized both in space and Euclidean time

Analytical description of instantons with fermionic back reaction (1)

$$S = \frac{\sum_{x,\tau} (\varphi_x^\tau)^2}{2U\Delta\tau} - \ln\det\left(I + \prod_\tau e^{-\Delta\tau H}\{e^{i\varphi_x^\tau}\}\right) -$$

$$- \ln\det\left(I + \prod_\tau e^{-\Delta\tau H}\{e^{-i\varphi_x^\tau}\}\right)$$

$$\frac{\partial S}{\partial \varphi_x^\tau} = \frac{\varphi_x^\tau}{U\Delta\tau} - \left[\bar{g}_{xx}^\tau i e^{i\varphi_x^\tau} - i(\bar{g}_{xx}^\tau)^* e^{-i\varphi_x^\tau}\right] = 0$$

(saddle point)

$\Rightarrow$ we need to add equations for g_{xx}^τ to close the system:

$$\bar{g}^{\tau+1} = \{e^{-i\varphi_x^{\tau+1}}\} e^{\Delta\tau H} \bar{g}^\tau \{e^{i\varphi_x^\tau}\} e^{-\Delta\tau H}$$

$$\Rightarrow \varphi_x^\tau = -U \,\mathrm{Im}\, \bar{g}_{xx}^\tau$$

Analytical description of instantons with fermionic back reaction (2)

Final system of equations for propagator in continuous time:

$$\boxed{\varphi_x^{\tau} = -U\,\mathrm{Im}\,\bar{g}^{\tau}_{xx}}$$

$$\begin{cases} \dot{\bar{g}}_{xx}(\tau) = -\varkappa \sum\limits_{\langle x,y\rangle} \left(\bar{g}_{xy} - \bar{g}_{yx}\right) \\ \dot{\bar{g}}_{xy}(\tau) = iU\,\bar{g}_{xy}\left(\mathrm{Im}\,\bar{g}_{xx} - \mathrm{Im}\,\bar{g}_{yy}\right) - \varkappa\left(\sum\limits_{\langle z_1,y\rangle} \bar{g}_{xz_1} - \sum\limits_{\langle z_2,x\rangle} \bar{g}_{z_2 y}\right) \end{cases}$$

Same equations can be obtained from

$$\frac{d\hat{A}}{d\tau} = [\hat{H}, \hat{A}]; \quad \hat{A} = \hat{a}^+_x a_y; \quad \hat{b}^+_x b_y; \text{ etc.}$$

$$\begin{cases} \dfrac{d(\hat{a}^+_x \hat{a}_x)}{d\tau} = -\varkappa \sum\limits_{x,y} \left(\hat{a}^+_y \hat{a}_x - \hat{a}^+_x \hat{a}_y\right) \\ \dfrac{d(\hat{a}^+_x \hat{a}_y)}{d\tau} = U\,\hat{a}^+_y \hat{a}_x \left(\hat{b}^+_x \hat{b}_x - \hat{b}^+_y b_y\right) - \varkappa\left(\sum\limits_{\langle z_1,y\rangle} \hat{a}^+_{z_1} \hat{a}_x - \sum\limits_{\langle z_2, x\rangle} \hat{a}^+_y \hat{a}_{z_2}\right) \end{cases}$$

Under minor appoximations, can be solved exactly, leads to the equations of physical pendulum with explicit solution through elliptical integrals

Mean field approximation: $\langle \hat{a}^+_x \hat{a}_y \hat{b}_x \hat{b}_x \rangle = g_{xy}\, g^*_{yy}$

Hessians and continuum limit

Degenerate saddle:

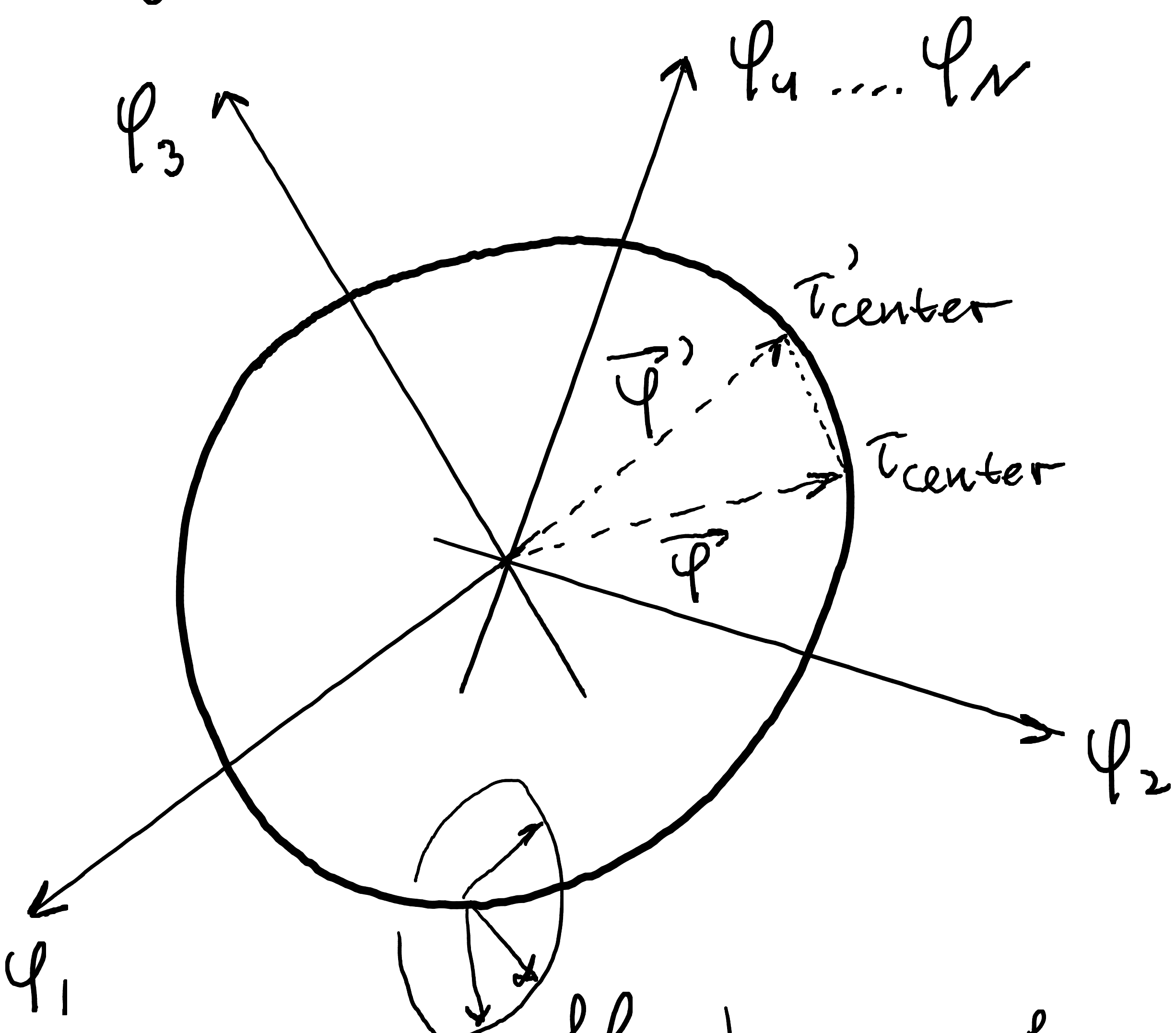

$\mathcal{H}_\perp$ - hessian for fluctuations in perpendicular directions

det $\mathcal{H}_\perp$ is dependent on $\Delta\tau$

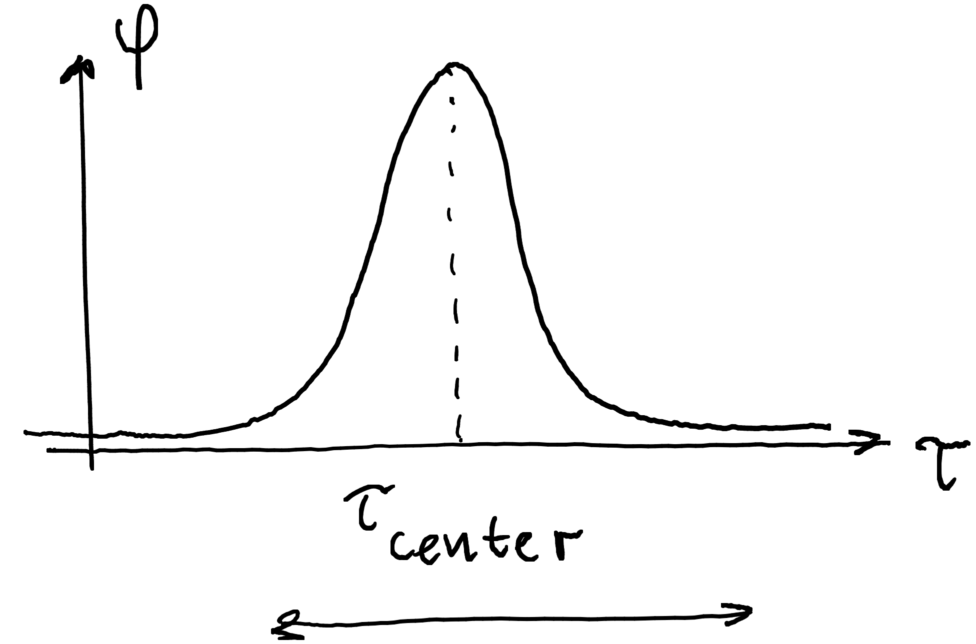

continuous symmetry: zero mode in hessian $\mathcal{H}$

$$L = N_\tau \left| \vec{\varphi}(\tau_c) - \vec{\varphi}(\tau_c + 1) \right| \Rightarrow$$

dependent on $\Delta\tau$

However:

$\boxed{L \left(\det \mathcal{H}_\perp \right)^{-1/2}}$ is $\Delta\tau$-independent

Interaction of instantons: several factors

1) Variation of action depending on relative position of the instantons
2) Variation of the determinant of Hessian
3) Variation of the volume element along the directions defined by zero modes (obtained by triangulation inside many-dimensional orbits)

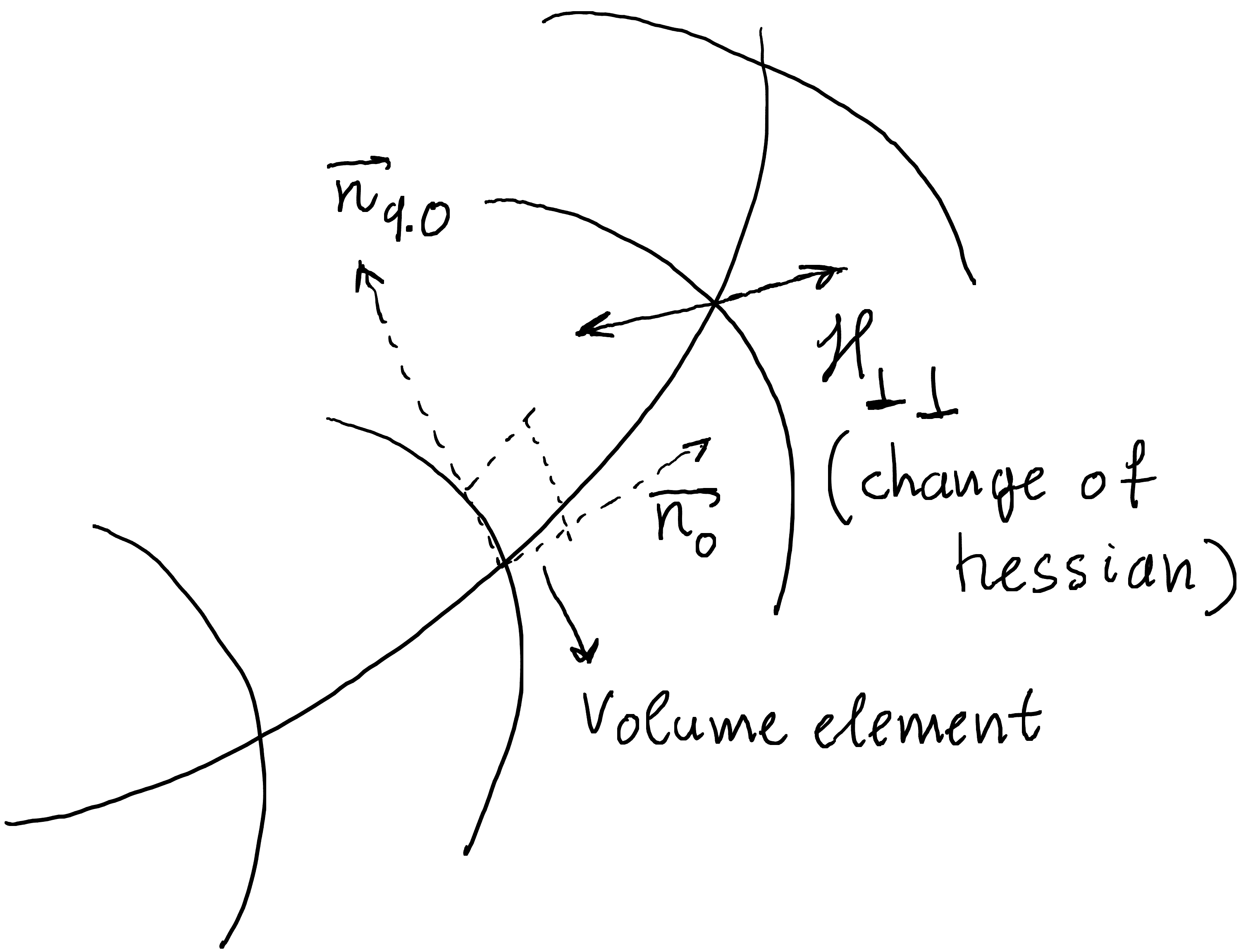

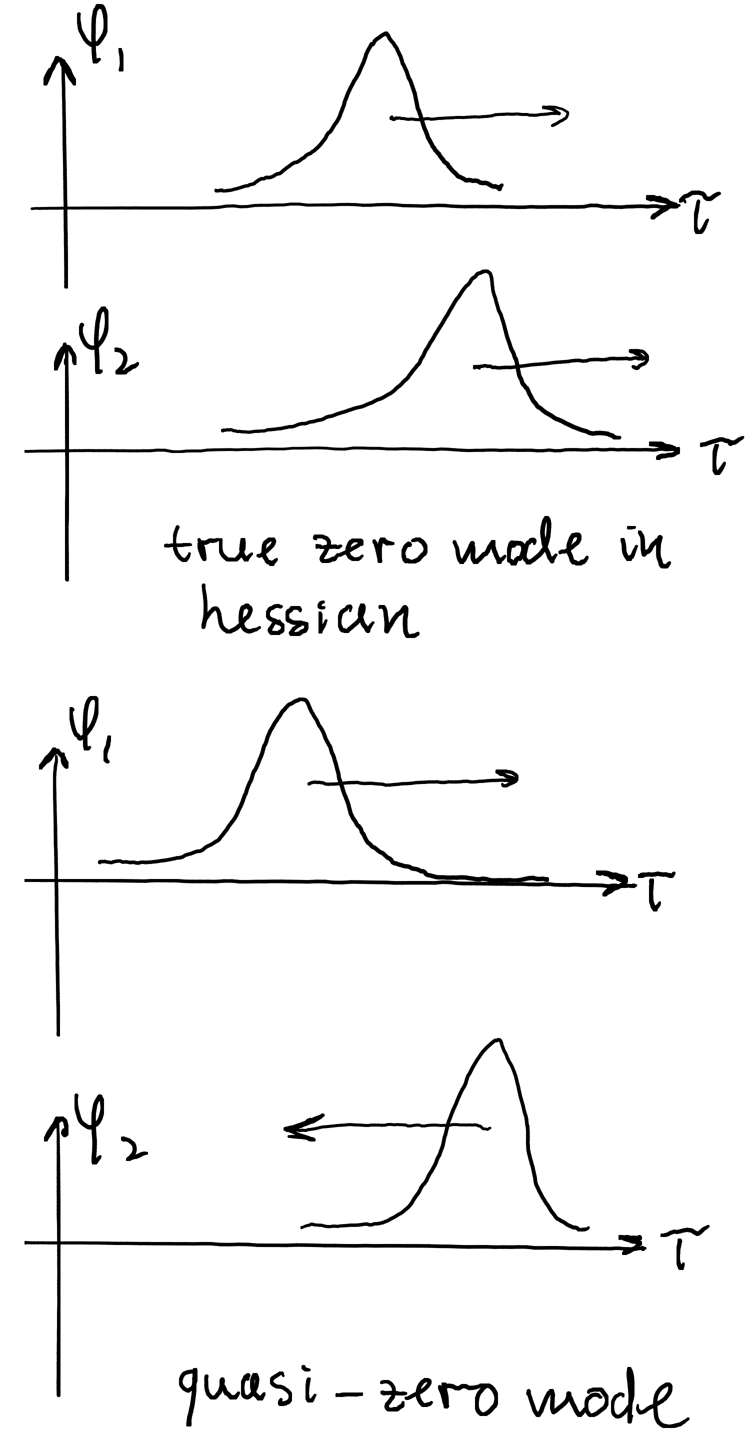

Examples of interaction curves

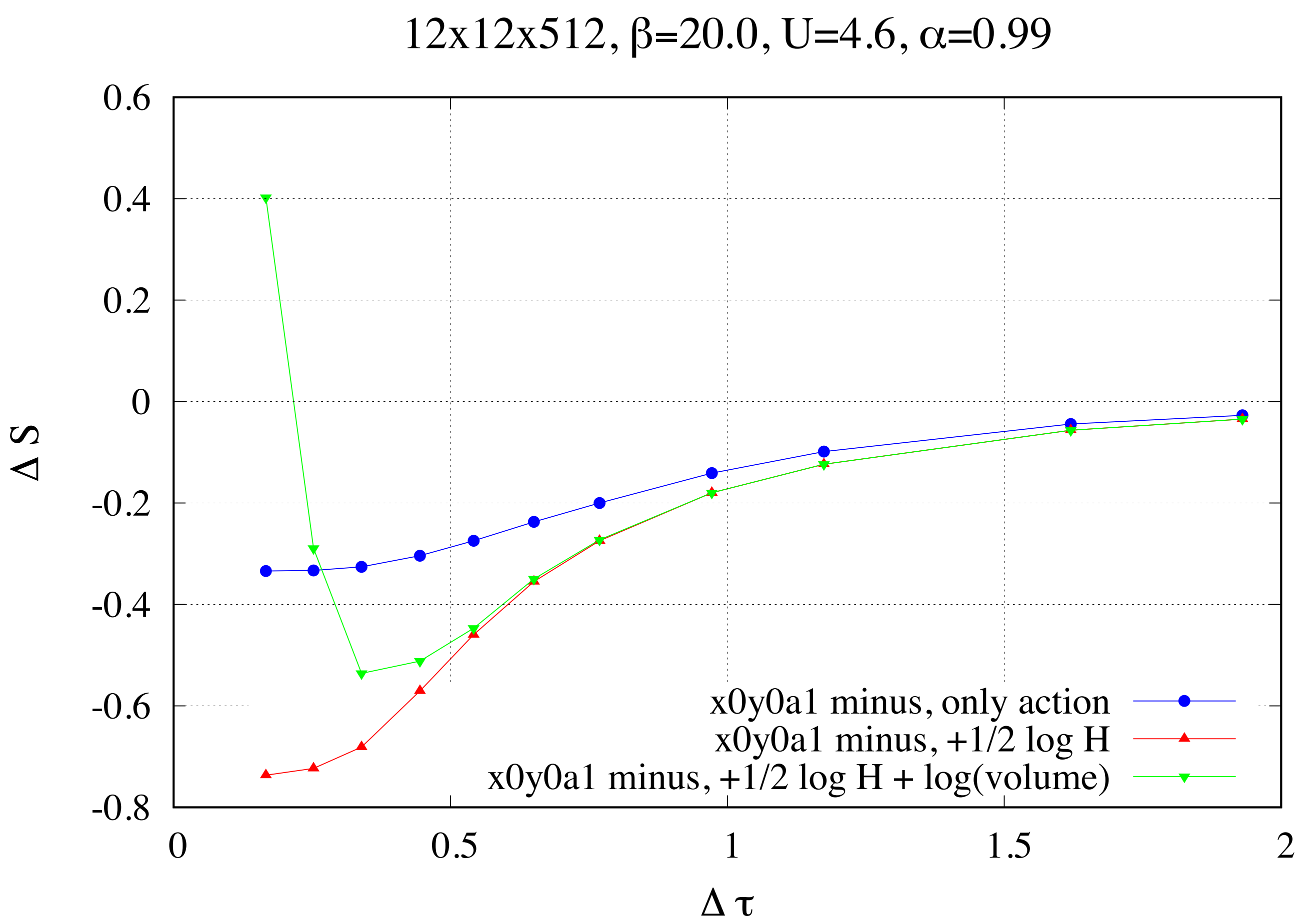

Instanton and anti-instanton at nearest-neighbour lattice sites

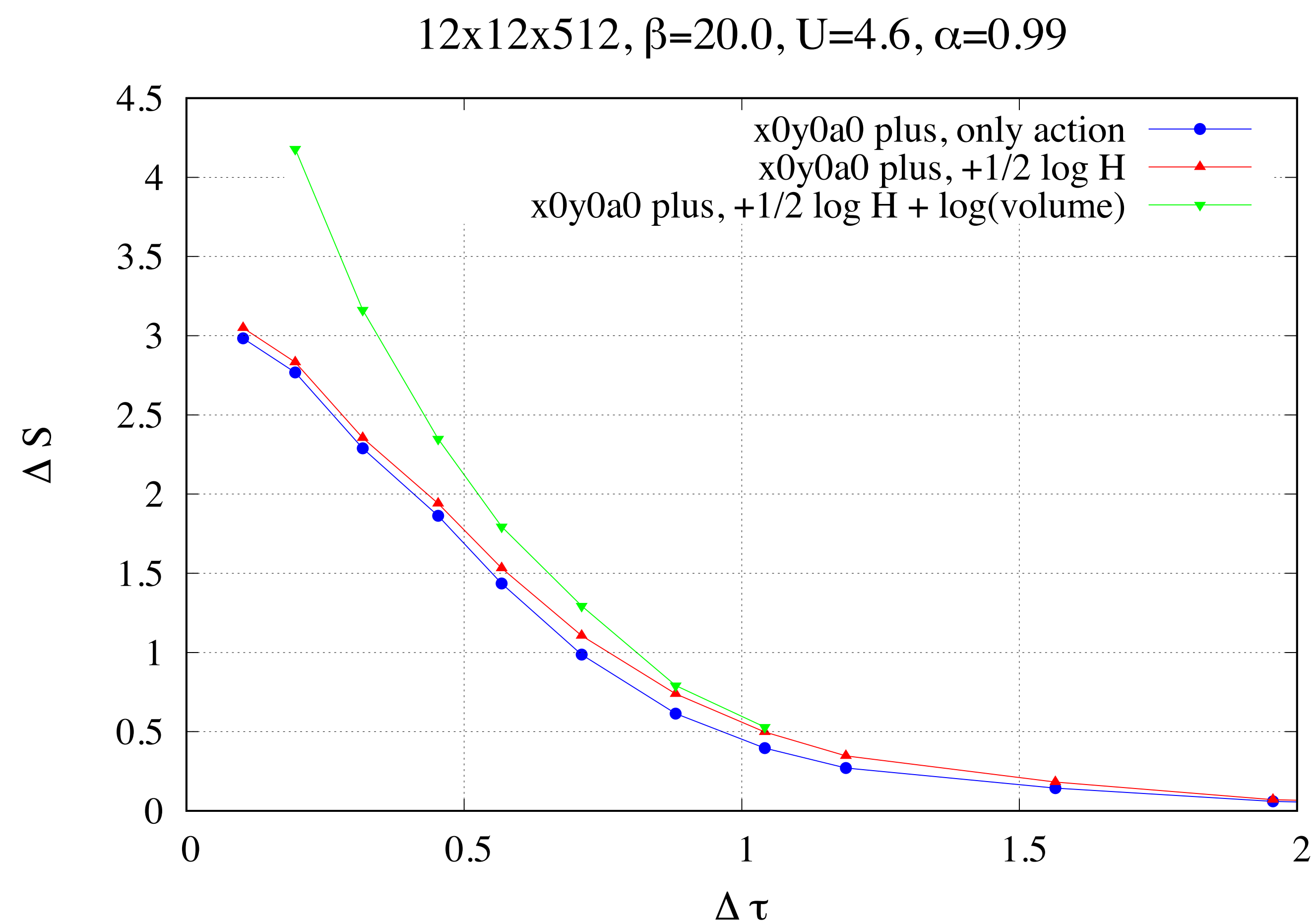

Two instantons at the same lattice site

Now we can construct several instanton gas models:

1) Analytical model using «hard spheres» approach, without taking into account lattice structure at all
2) Classical Monte Carlo for the simple hardcore repulsion interaction
3) Classical Monte Carlo for the model with full interaction profiles

Simple analytic partition function for non-interacting instantons (1)

All N-instanton saddle points + gaussian fluctuations around them.

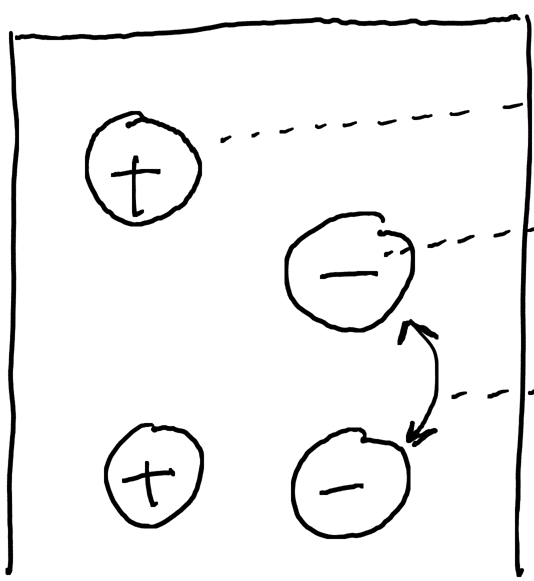

→ instanton

→ anti-instanton

→ can not occupy the same volume in space and Euclidean time:

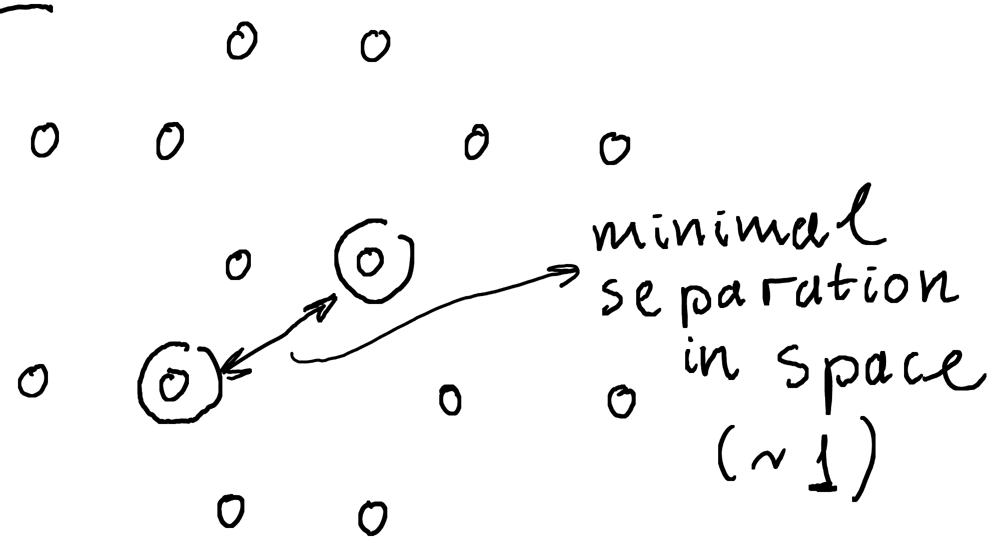

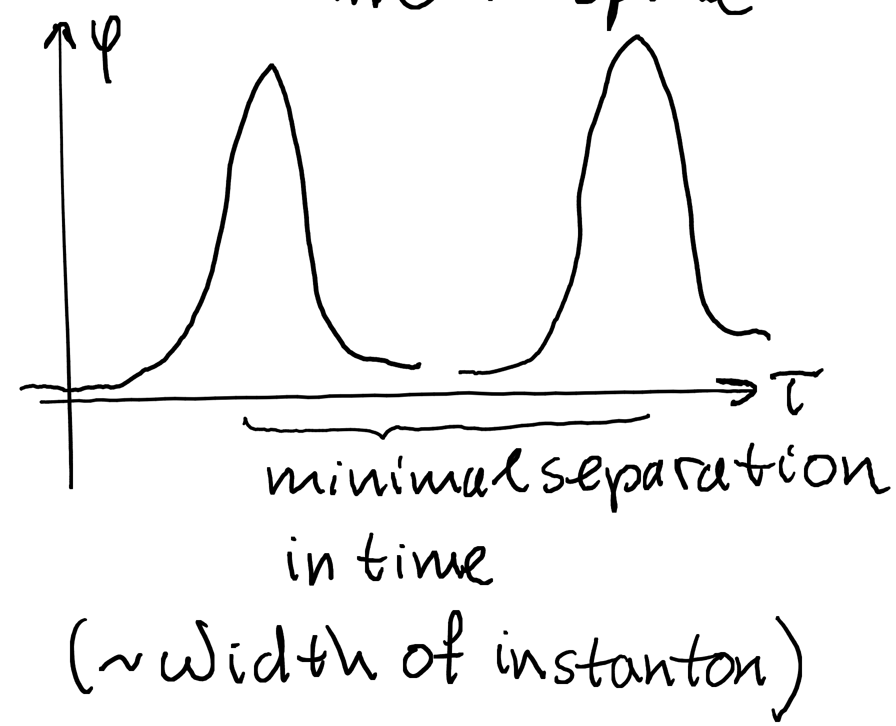

Simple analytic partition function for non-interacting instantons (2)

$$\frac{Z}{Z_0} = 1 + \sum_{K=1}^{K_{max}} \frac{1}{K!} \underbrace{\beta N_s (\beta N_s - \Delta\beta X) \ldots (\beta N_s - (K-1)\Delta\beta X)}_{\text{Volume factors}} \times$$

Z_0: vacuum

$\frac{1}{K!}$: equivalence of instantons

$$\times 2^{2K} e^{-S_0 K} \left(\left(\frac{\det \mathcal{H}_0}{2\pi \det \mathcal{H}_\perp} \right)^{\frac{1}{2}} \frac{L}{\beta} \right)^K$$

S_0: quantum of action

L: length of orbit in configuration space

2^{2K}: combinatorial factor: Sublattice + (instanton-anti-instanton)

$$K_{max} \cong \frac{\beta}{\Delta\beta} \frac{N_s}{X}$$

$$\Rightarrow f = f_0 - \frac{1}{\Delta\beta X} \ln \left(1 + \frac{4 e^{-S_0} \Delta\beta X L}{\beta \sqrt{\det \mathcal{H}_\perp \det \mathcal{H}_0 \cdot 2\pi}} \right)$$

f_0: vacuum

Benchmark: distribution of instantons

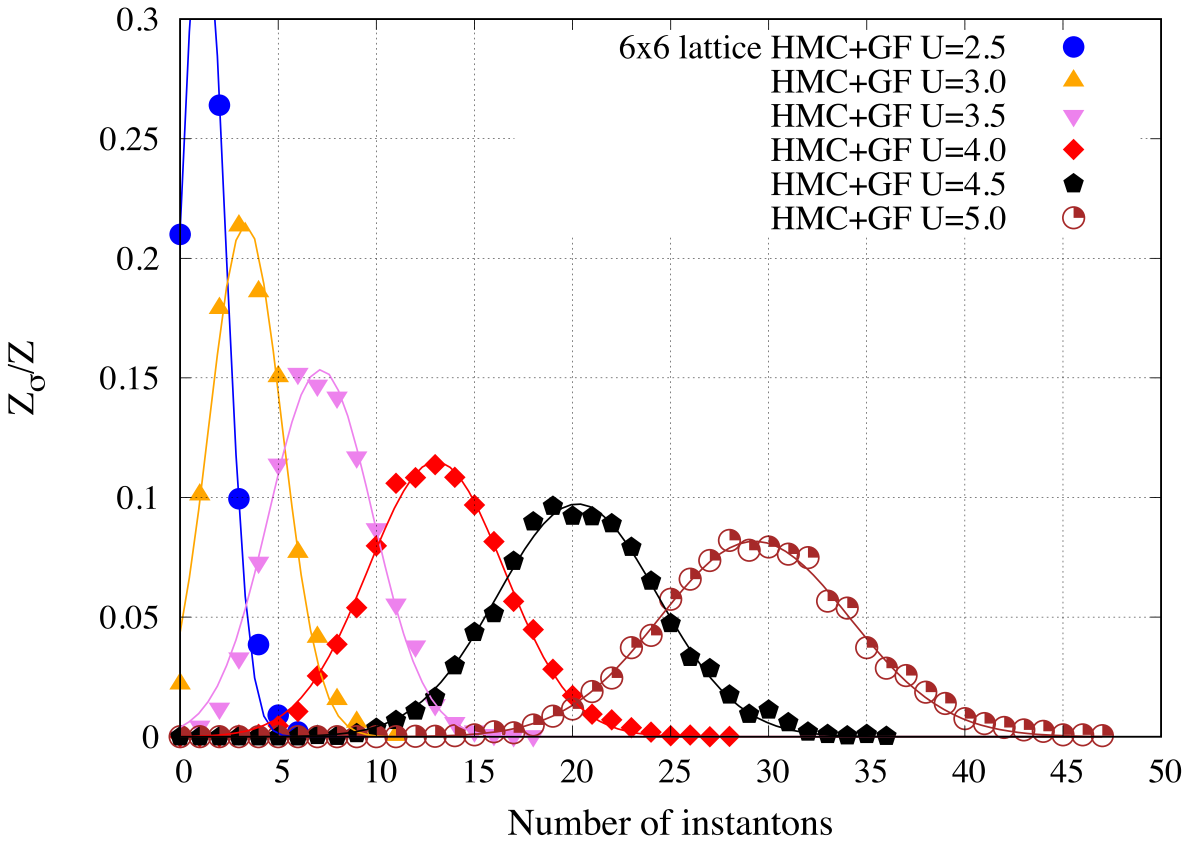

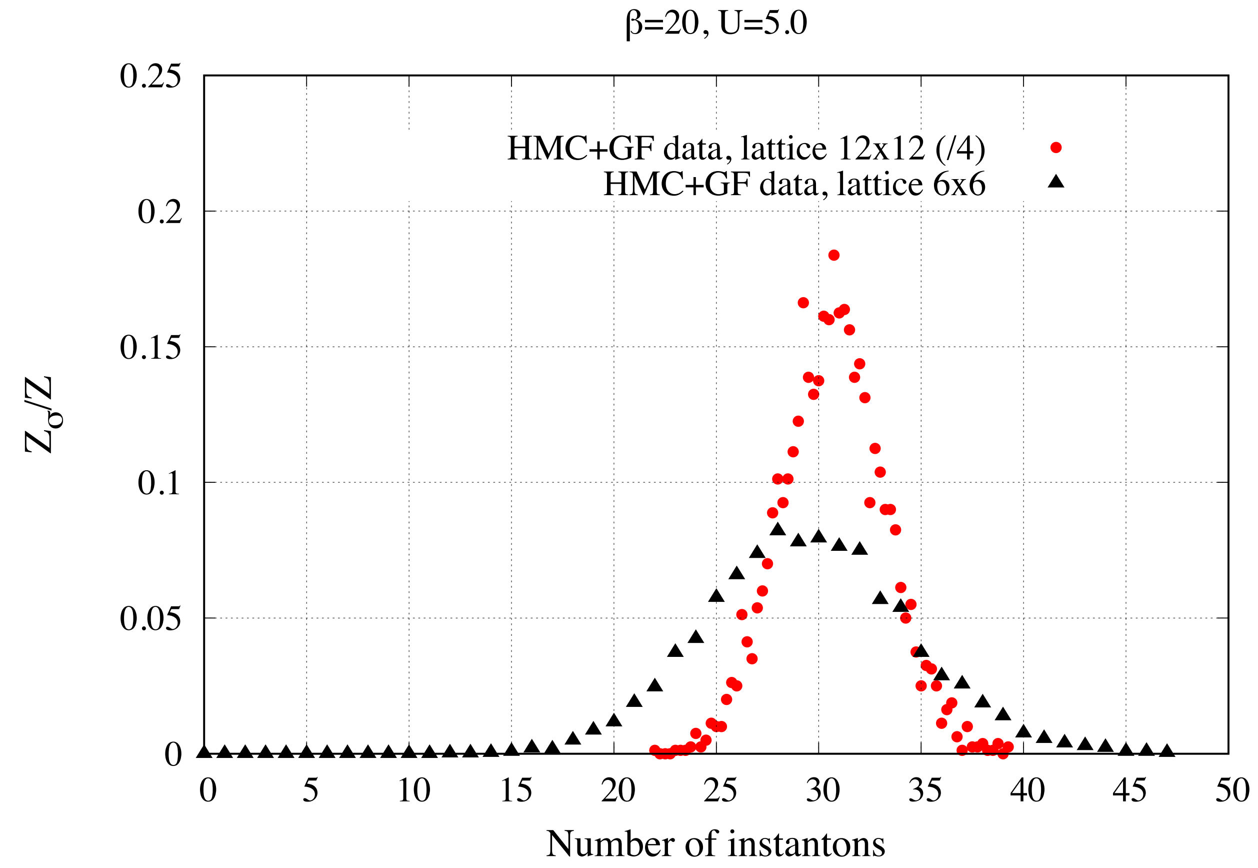

Distribution for the number of instantons and its comparison vs analytical and classical MC predictions:

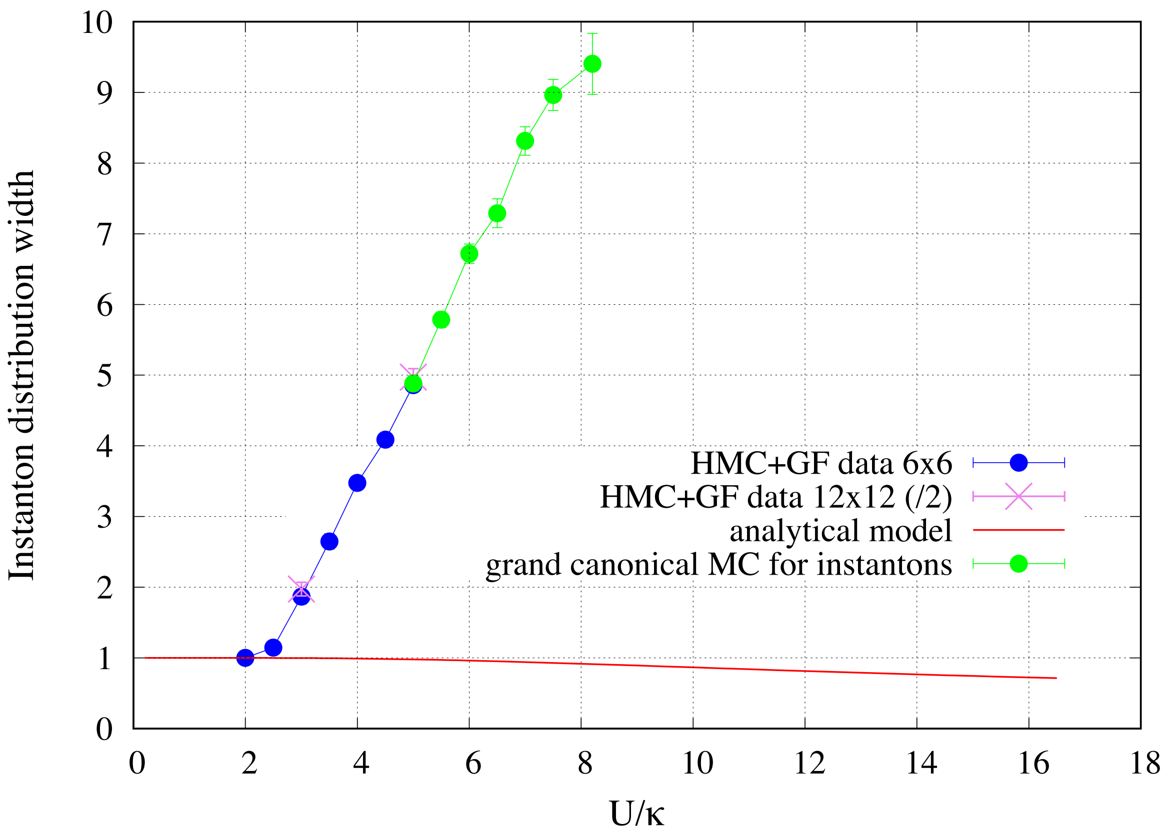

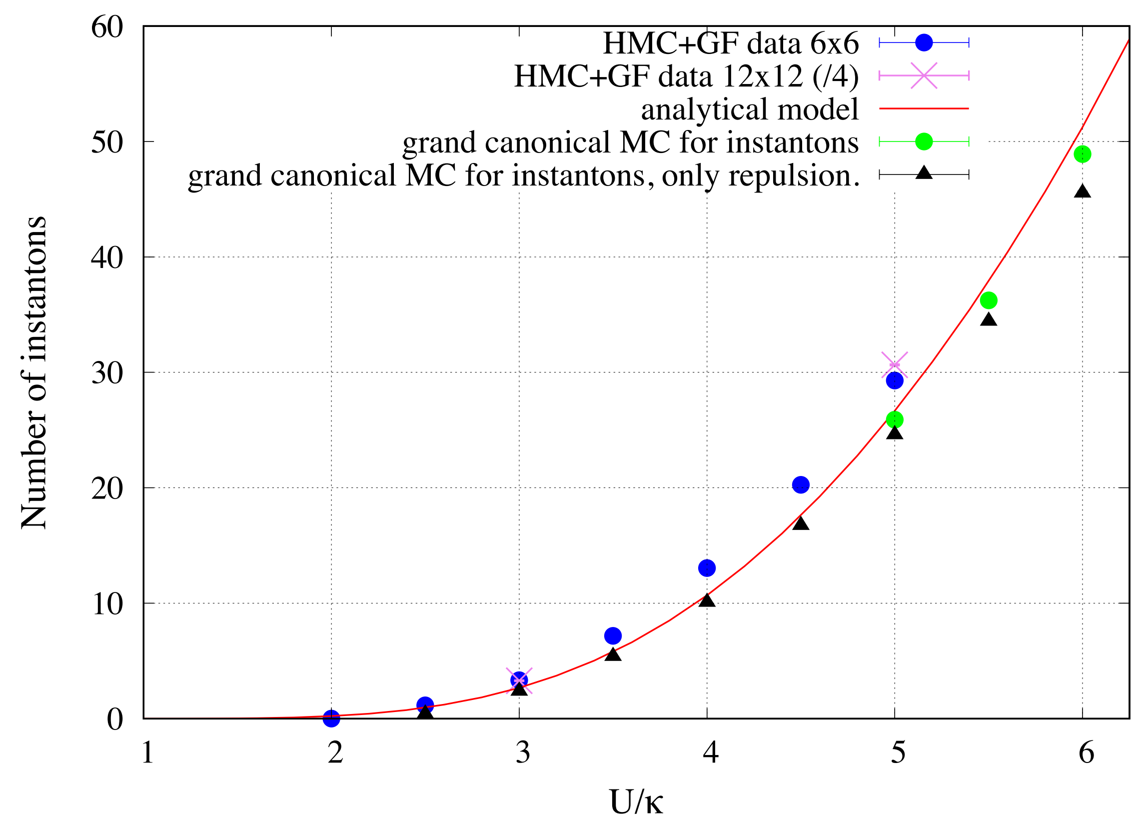

Physics from weakly interacting instanton gas model

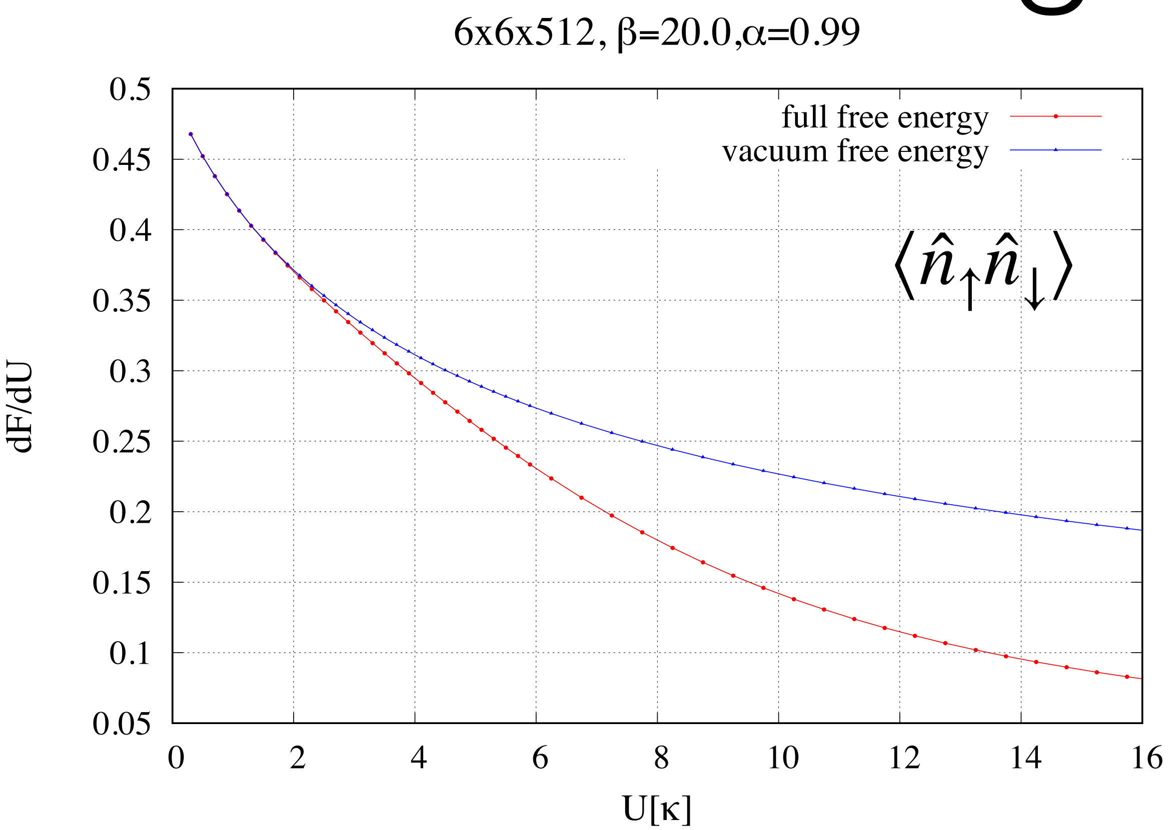

Double occupancy

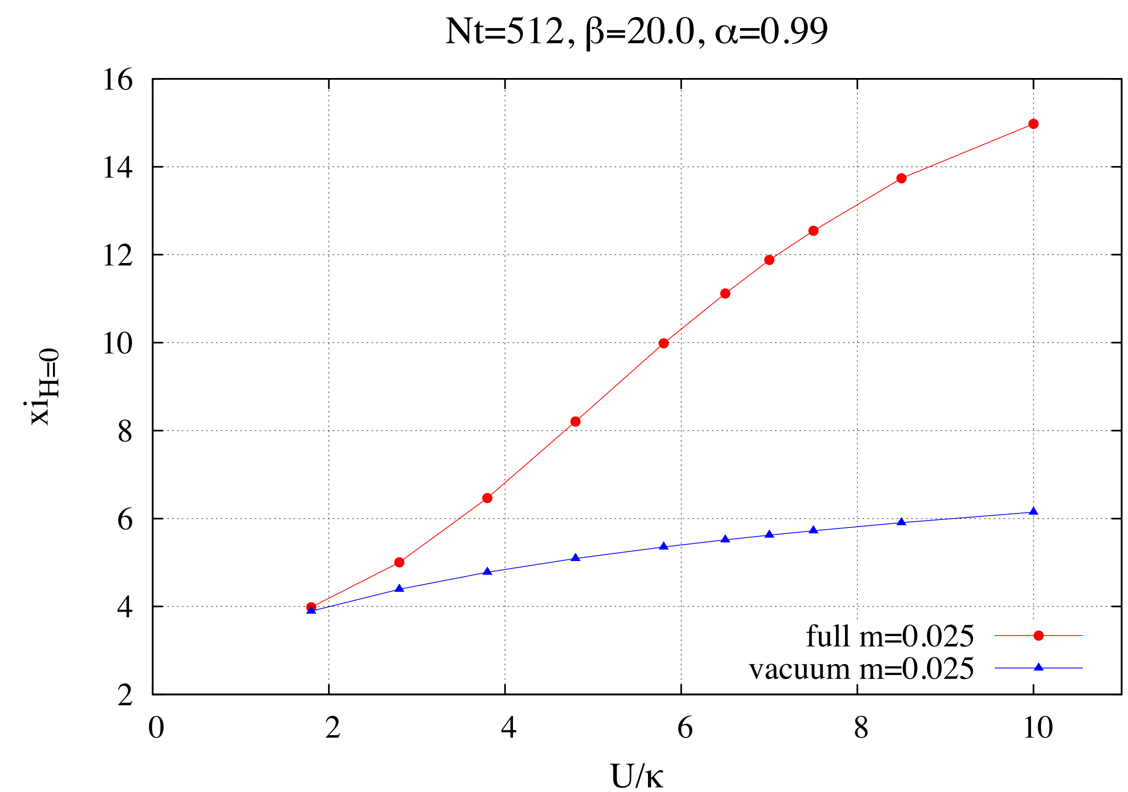

Magnetic susceptibility doesn't diverge at any point: no description of the phase transition (AFM spin ordering)

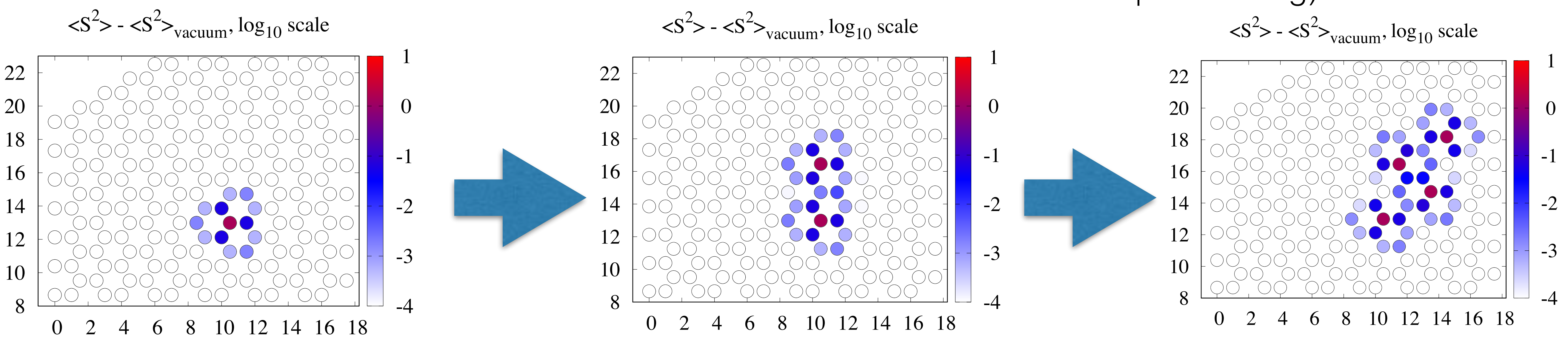

We really described spin localization, but local spins are still in paramagnetic phase

Beyond Gaussian approximation: full integration over one dominant thimble

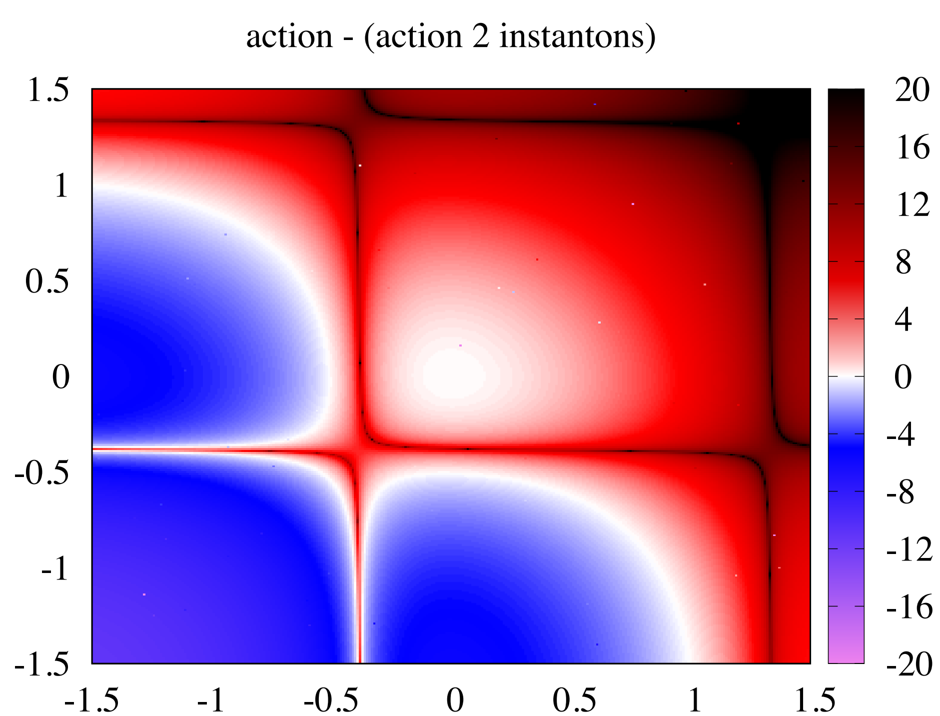

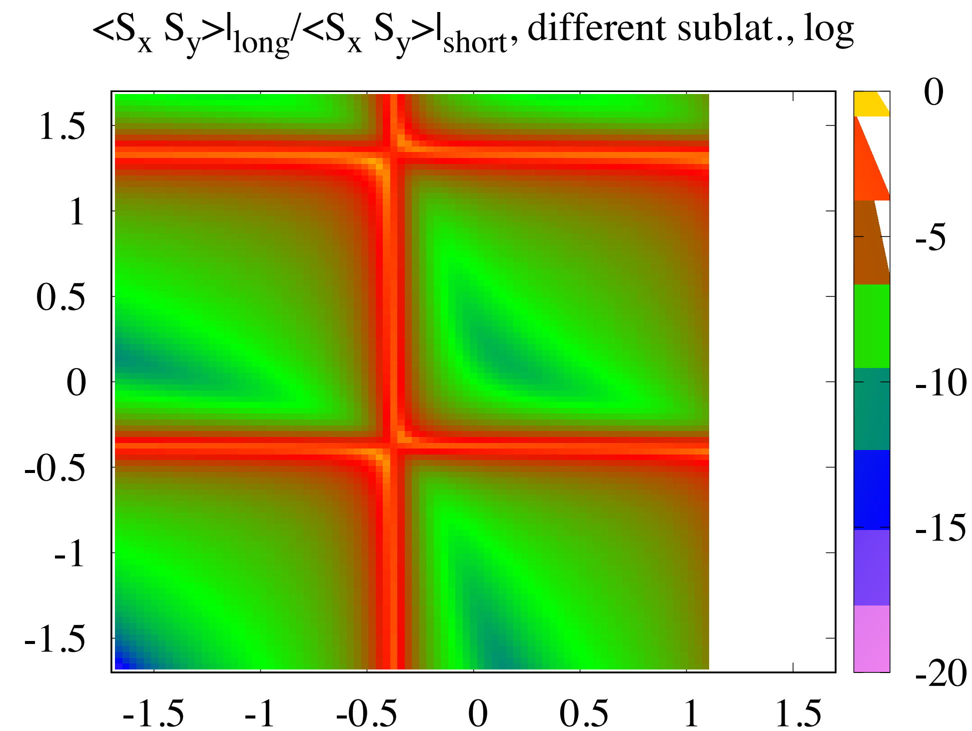

Propagator diverges at the zeros of determinant, thus fermonic observables increase

IMPORTANT: the form of dominant saddle is taken from classical MC for instanton gas

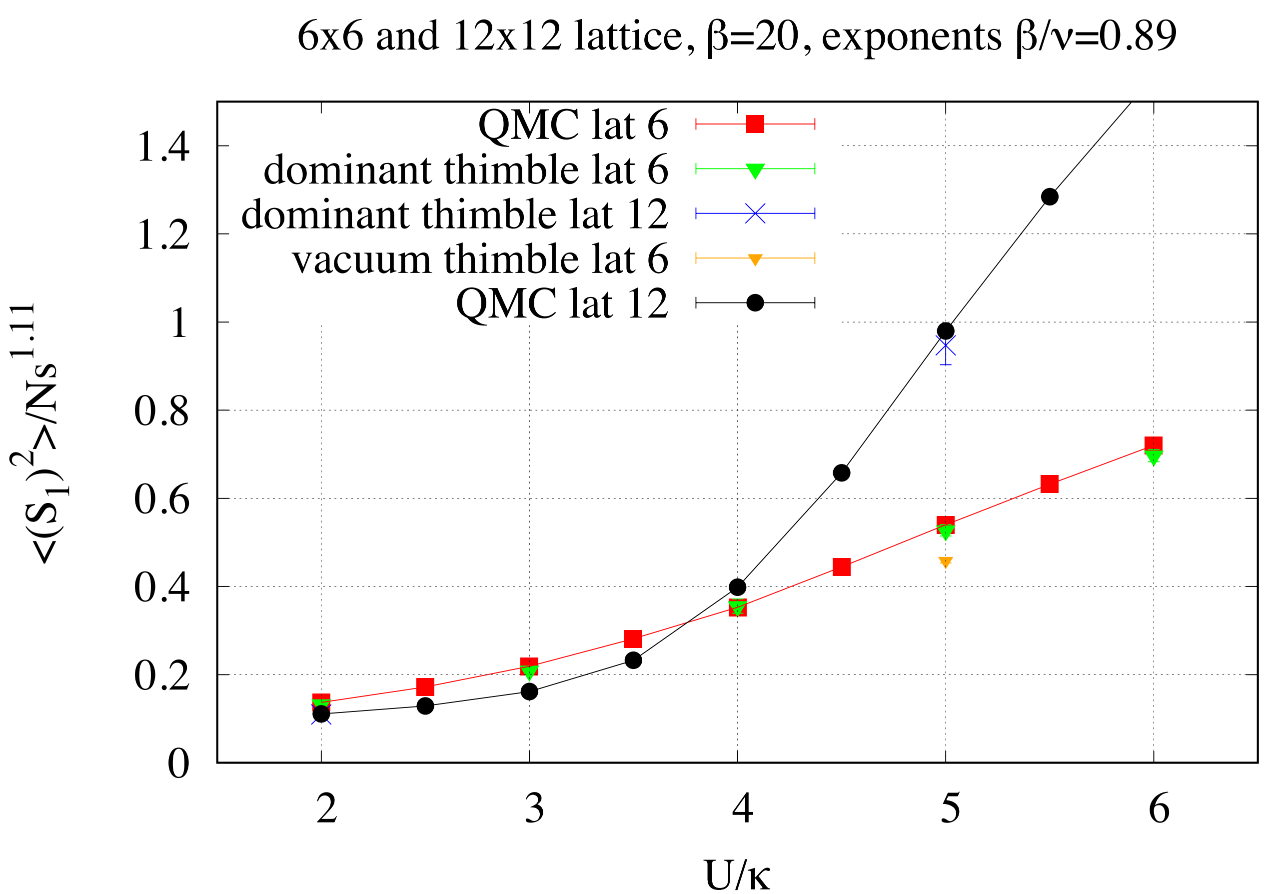

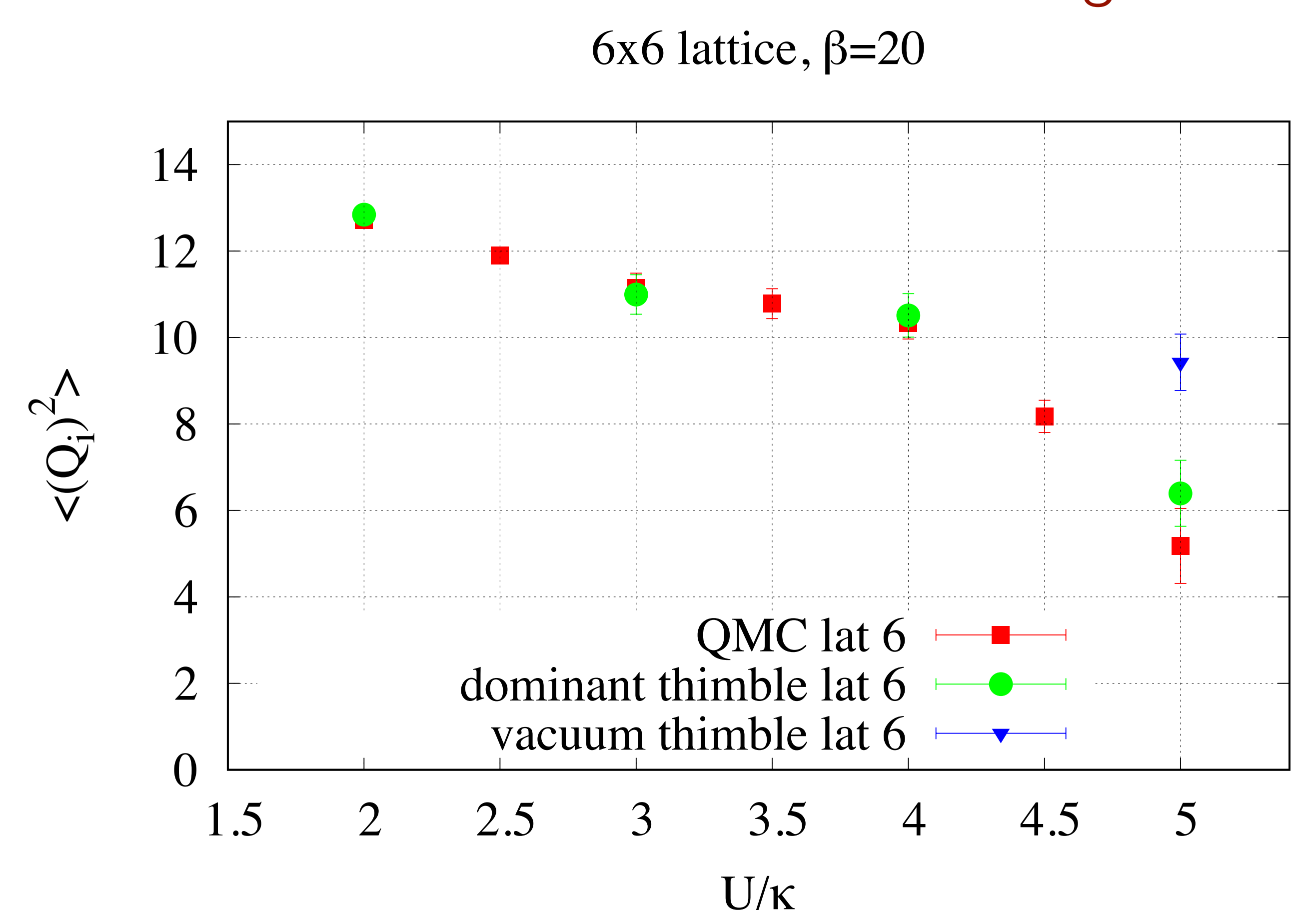

Further perspectives

Saddle points in complex space away of half-filling: instantons are still localized in space-time, but we need to take into account imaginary parts of the fields

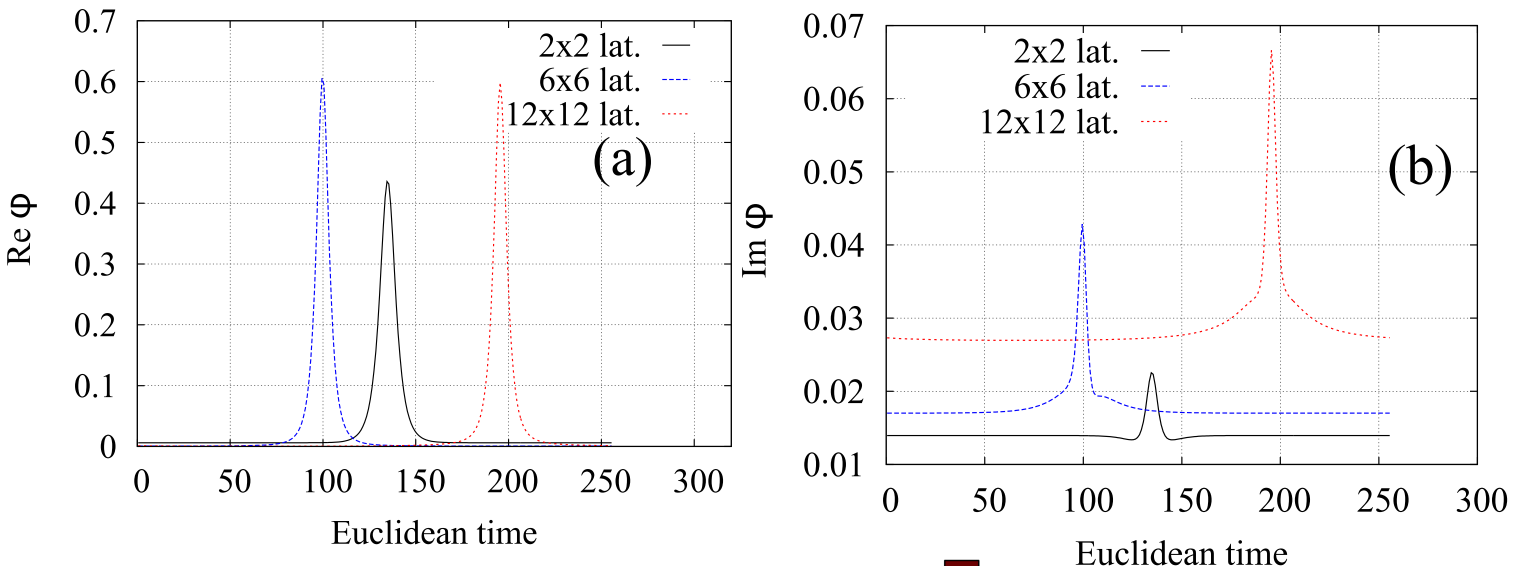

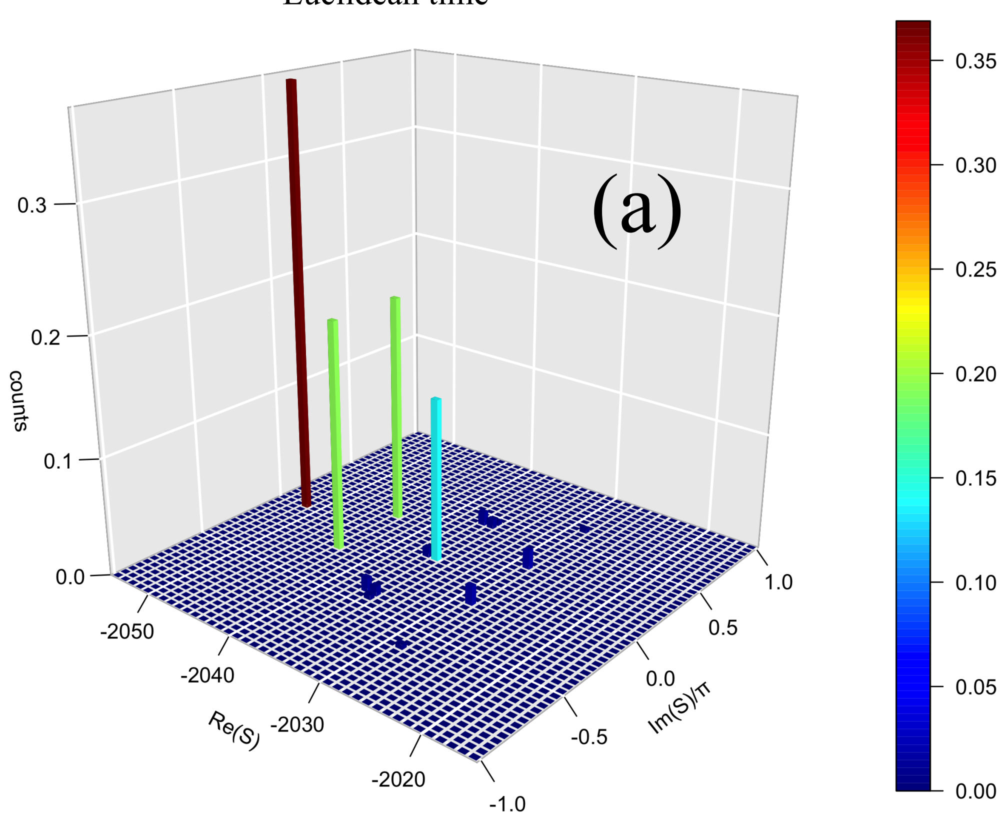

We can still predict with classical MC, which saddle to pick up for the integral over dominant thimble

Another models: e.g. square lattice Hubbard model features not only localized instantons but also domain walls as saddles points

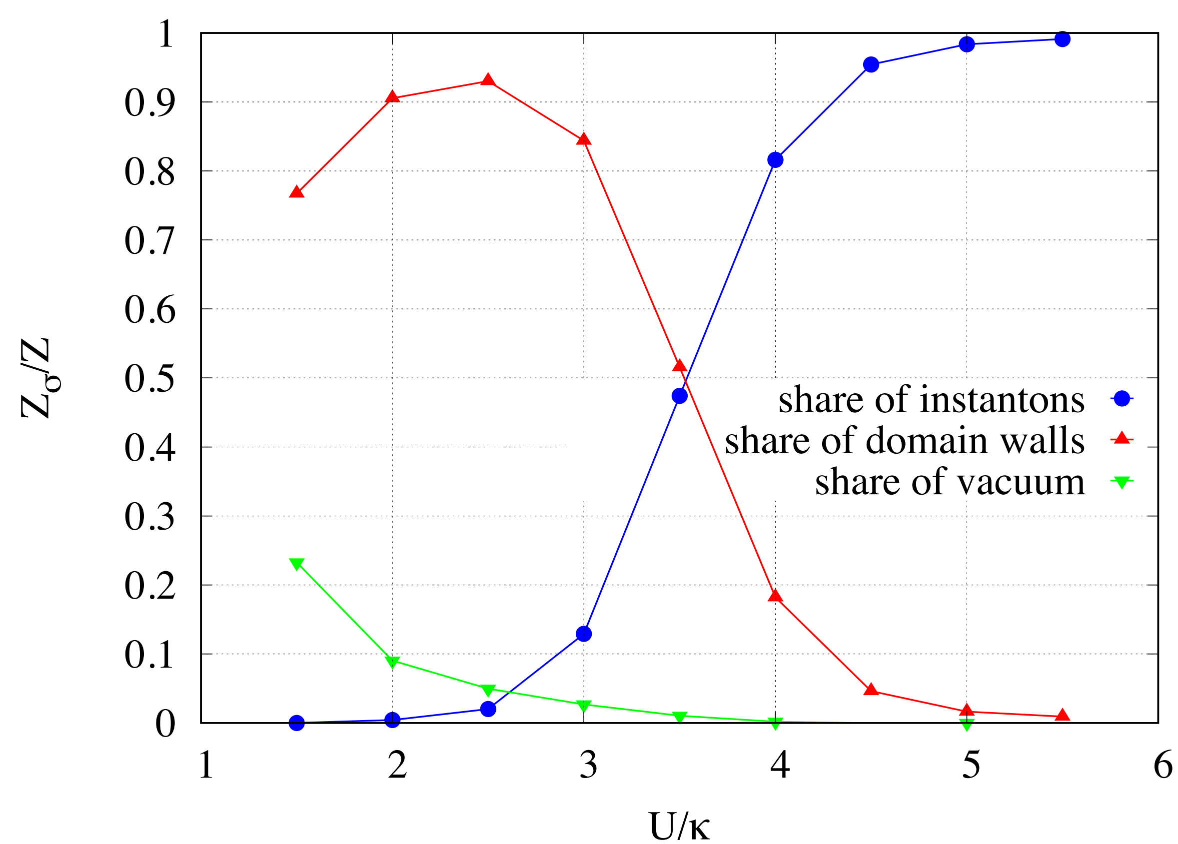

Summary

- In the absence of the sign problem, we can find all important saddle points of the full action, by solving GF equations and taking into account fermionic determinant. This solution can be accomplished using non-iterative Schur complement solver for the calculation of exact fermionic forces.
- With this information, we demonstrate the construction of the saddle point approximations considering Gaussian fluctuations around the saddles. Hubbard model on hexagonal lattice is taken as an example. Saddle points can be viewed as instantons with the back-reaction from fermions inserted in the Euclidean field equations. We can reproduce the real density of instantons with 10% precision.
- Even simple instanton gas model already features at least some important properties of the initial quantum Hamiltonian: spin localization and the growth of magnetic susceptibility. However, in order to describe the phase transition one needs to perform the full integration over thimble to take into account configurations in the vicinity of zeros of the fermionic determinant.
- We show that it is enough to perform integral over only one dominant thimble, and corresponding saddle point can be found using classical grand-canonical MC for instanton gas model.
- Since the saddle points do not change qualitatively away of half-filling, we can try to expand this model to non-zero chemical potential, where QMC doesn’t work due to the sign problem. In this case the instanton gas model provides correct starting saddle point for Lefschetz thimbles algorithms.